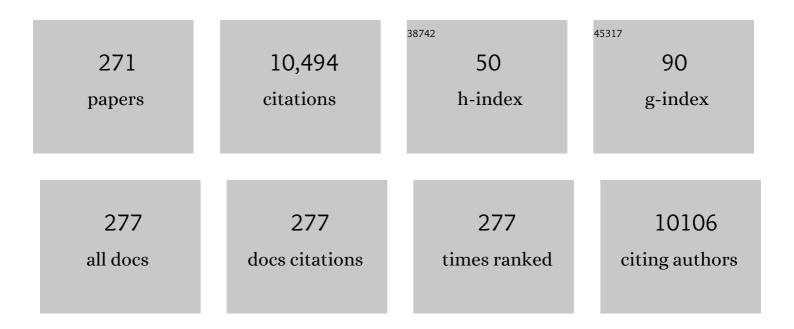
List of Publications by Year in descending order

Source: https://exaly.com/author-pdf/7310570/publications.pdf Version: 2024-02-01



LOON REOM SEO

#	Article	IF	CITATIONS
1	Application of computer-aided diagnosis for Lung-RADS categorization in CT screening for lung cancer: effect on inter-reader agreement. European Radiology, 2022, 32, 1054-1064.	4.5	10
2	Identification of predictors for brain metastasis in newly diagnosed non-small cell lung cancer: a single-center cohort study. European Radiology, 2022, 32, 990-1001.	4.5	5
3	Learning Curve for CT-Guided Percutaneous Transthoracic Needle Biopsy: Retrospective Evaluation Among 17 Thoracic Imaging Fellows at a Tertiary Referral Hospital. American Journal of Roentgenology, 2022, 218, 112-123.	2.2	6
4	Content-based Image Retrieval by Using Deep Learning for Interstitial Lung Disease Diagnosis with Chest CT. Radiology, 2022, 302, 187-197.	7.3	56
5	Utility of a Deep Learning Algorithm for Detection of Reticular Opacity on Chest Radiography in Patients With Interstitial Lung Disease. American Journal of Roentgenology, 2022, 218, 642-650.	2.2	9
6	Multi-task vision transformer using low-level chest X-ray feature corpus for COVID-19 diagnosis and severity quantification. Medical Image Analysis, 2022, 75, 102299.	11.6	69
7	Volume Doubling Times of Pulmonary Metastases in Patients With Bone and Soft-Tissue Sarcomas: Associations With Subsequent New Metastases and Survival After Metastasectomy. American Journal of Roentgenology, 2022, 218, 624-632.	2.2	3
8	Differences in the prognostic implication of ground-glass opacity on CT according to pathological nodal status in lung cancers treated with lobectomy or pneumonectomy. European Radiology, 2022, 32, 4405-4413.	4.5	5
9	Prognosis for Pneumonic-Type Invasive Mucinous Adenocarcinoma in a Single Lobe on CT: Is It Reasonable to Designate It as Clinical T3?. Korean Journal of Radiology, 2022, 23, 370.	3.4	4
10	Utilizing Synthetic Nodules for Improving Nodule Detection in Chest Radiographs. Journal of Digital Imaging, 2022, , 1.	2.9	4
11	<i>BJR</i> functional imaging of the lung special feature: introductory editorial. British Journal of Radiology, 2022, 95, 20229004.	2.2	0
12	Deep chest <scp>Xâ€ray</scp> : Detection and classification of lesions based on deep convolutional neural networks. International Journal of Imaging Systems and Technology, 2021, 31, 72-81.	4.1	5
13	Performance of radiomics models for survival prediction in non-small-cell lung cancer: influence of CT slice thickness. European Radiology, 2021, 31, 2856-2865.	4.5	11
14	Breast-conserving surgery with 3D-printed surgical guide: a single-center, prospective clinical study. Scientific Reports, 2021, 11, 2252.	3.3	10
15	Content-Based Image Retrieval of Chest CT with Convolutional Neural Network for Diffuse Interstitial Lung Disease: Performance Assessment in Three Major Idiopathic Interstitial Pneumonias. Korean Journal of Radiology, 2021, 22, 281.	3.4	18
16	Use of Artificial Intelligence-Based Software as Medical Devices for Chest Radiography: A Position Paper from the Korean Society of Thoracic Radiology. Korean Journal of Radiology, 2021, 22, 1743.	3.4	29
17	New Method for Combined Quantitative Assessment of Air-Trapping and Emphysema on Chest Computed Tomography in Chronic Obstructive Pulmonary Disease: Comparison with Parametric Response Mapping. Korean Journal of Radiology, 2021, 22, 1719.	3.4	8
18	Usefulness of 3D-surgical guides in breast conserving surgery after neoadjuvant treatment. Scientific Reports, 2021, 11, 3376.	3.3	7

#	Article	IF	CITATIONS
19	Deep learning–based differentiation of invasive adenocarcinomas from preinvasive or minimally invasive lesions among pulmonary subsolid nodules. European Radiology, 2021, 31, 6239-6247.	4.5	8
20	Use of a Commercially Available Deep Learning Algorithm to Measure the Solid Portions of Lung Cancer Manifesting as Subsolid Lesions at CT: Comparisons with Radiologists and Invasive Component Size at Pathologic Examination. Radiology, 2021, 299, 202-210.	7.3	15
21	Radiomics approach for survival prediction in chronic obstructive pulmonary disease. European Radiology, 2021, 31, 7316-7324.	4.5	11
22	Computer-aided Detection of Subsolid Nodules at Chest CT: Improved Performance with Deep Learning–based CT Section Thickness Reduction. Radiology, 2021, 299, 211-219.	7.3	11
23	Added Value of Deep Learning–based Detection System for Multiple Major Findings on Chest Radiographs: A Randomized Crossover Study. Radiology, 2021, 299, 450-459.	7.3	42
24	Pulmonary Functional Imaging: Part 2—State-of-the-Art Clinical Applications and Opportunities for Improved Patient Care. Radiology, 2021, 299, 524-538.	7.3	29
25	Predicting long-term mortality with two different criteria of exercise-induced desaturation in COPD. Respiratory Medicine, 2021, 182, 106393.	2.9	6
26	CT radiomics-based prediction of anaplastic lymphoma kinase and epidermal growth factor receptor mutations in lung adenocarcinoma. European Journal of Radiology, 2021, 139, 109710.	2.6	13
27	Pulmonary Functional Imaging: Part 1—State-of-the-Art Technical and Physiologic Underpinnings. Radiology, 2021, 299, 508-523.	7.3	29
28	Deep radiomics-based survival prediction in patients with chronic obstructive pulmonary disease. Scientific Reports, 2021, 11, 15144.	3.3	14
29	Prognostic performance in lung cancer according to tumor size: Comparison of axial, multiplanar, and 3-dimensional CT measurement to pathological size. European Journal of Radiology, 2021, 144, 109976.	2.6	0
30	Optimal number of strong labels for curriculum learning with convolutional neural network to classify pulmonary abnormalities in chest radiographs. Computers in Biology and Medicine, 2021, 136, 104750.	7.0	8
31	Lobar Ventilation in Patients with COPD Assessed with the Full-Scale Airway Network Flow Model and Xenon-enhanced Dual-Energy CT. Radiology, 2021, 298, 201-209.	7.3	5
32	Functional Assessment of COPD. Medical Radiology, 2021, , 125-151.	0.1	0
33	Image-Based Phenotyping, Deep Learning (DL), and Artificial Intelligence (AI) Applications in Clinical and Research Radiology and Chest Imaging. Medical Radiology, 2021, , 319-335.	0.1	0
34	Fully Automated Lung Lobe Segmentation in Volumetric Chest CT with 3D U-Net: Validation with Intra- and Extra-Datasets. Journal of Digital Imaging, 2020, 33, 221-230.	2.9	61
35	Development of a CT imaging phantom of anthromorphic lung using fused deposition modeling 3D printing. Medicine (United States), 2020, 99, e18617.	1.0	24
36	Deep learning-based detection system for multiclass lesions on chest radiographs: comparison with observer readings. European Radiology, 2020, 30, 1359-1368.	4.5	61

#	Article	IF	CITATIONS
37	Magnetic resonance imaging based 3-dimensional printed breast surgical guide for breast-conserving surgery in ductal carcinoma in situ: a clinical trial. Scientific Reports, 2020, 10, 18534.	3.3	8
38	Reproducibility of abnormality detection on chest radiographs using convolutional neural network in paired radiographs obtained within a short-term interval. Scientific Reports, 2020, 10, 17417.	3.3	9
39	Expanding Applications of Pulmonary MRI in the Clinical Evaluation of Lung Disorders: Fleischner Society Position Paper. Radiology, 2020, 297, 286-301.	7.3	95
40	CT kernel conversions using convolutional neural net for super-resolution with simplified squeeze-and-excitation blocks and progressive learning among smooth and sharp kernels. Computer Methods and Programs in Biomedicine, 2020, 196, 105615.	4.7	7
41	Interstitial lung abnormalities detected incidentally on CT: a Position Paper from the Fleischner Society. Lancet Respiratory Medicine,the, 2020, 8, 726-737.	10.7	279
42	Severe vitamin D deficiency is associated with emphysema progression in male patients with COPD. Respiratory Medicine, 2020, 163, 105890.	2.9	6
43	Outcome prediction in resectable lung adenocarcinoma patients: value of CT radiomics. European Radiology, 2020, 30, 4952-4963.	4.5	23
44	Optimal matrix size of chest radiographs for computer-aided detection on lung nodule or mass with deep learning. European Radiology, 2020, 30, 4943-4951.	4.5	17
45	Differentiation of predominant subtypes of lung adenocarcinoma using a quantitative radiomics approach on CT. European Radiology, 2020, 30, 4883-4892.	4.5	27
46	Volume Doubling Times of Lung Adenocarcinomas: Correlation with Predominant Histologic Subtypes and Prognosis. Radiology, 2020, 295, 703-712.	7.3	38
47	Assessment of the Robustness of Convolutional Neural Networks in Labeling Noise by Using Chest X-Ray Images From Multiple Centers. JMIR Medical Informatics, 2020, 8, e18089.	2.6	11
48	Artificial Intelligence in Health Care: Current Applications and Issues. Journal of Korean Medical Science, 2020, 35, e379.	2.5	46
49	Quantitative Vertebral Bone Density Seen on Chest CT in Chronic Obstructive Pulmonary Disease Patients: Association with Mortality in the Korean Obstructive Lung Disease Cohort. Korean Journal of Radiology, 2020, 21, 880.	3.4	6
50	Visual and Quantitative Assessments of Regional Xenon-Ventilation Using Dual-Energy CT in Asthma-Chronic Obstructive Pulmonary Disease Overlap Syndrome: A Comparison with Chronic Obstructive Pulmonary Disease. Korean Journal of Radiology, 2020, 21, 1104.	3.4	10
51	Prognostic value of radiomic analysis of iodine overlay maps from dual-energy computed tomography in patients with resectable lung cancer. European Radiology, 2019, 29, 915-923.	4.5	29
52	Low morphometric complexity of emphysematous lesions predicts survival in chronic obstructive pulmonary disease patients. European Radiology, 2019, 29, 176-185.	4.5	4
53	Effects of emphysema on physiological and prognostic characteristics of lung function in idiopathic pulmonary fibrosis. Respirology, 2019, 24, 55-62.	2.3	24
54	Lung Segmentation on HRCT and Volumetric CT for Diffuse Interstitial Lung Disease Using Deep Convolutional Neural Networks. Journal of Digital Imaging, 2019, 32, 1019-1026.	2.9	79

#	Article	IF	CITATIONS
55	MRI-based 3D-printed surgical guides for breast cancer patients who received neoadjuvant chemotherapy. Scientific Reports, 2019, 9, 11991.	3.3	17
56	Utility of Computed Tomography in a Differential Diagnosis for the Patients with an Initial Diagnosis of Chronic Obstructive Pulmonary Disease Exacerbation. Tuberculosis and Respiratory Diseases, 2019, 82, 234.	1.8	10
57	Deep Learning–based Image Conversion of CT Reconstruction Kernels Improves Radiomics Reproducibility for Pulmonary Nodules or Masses. Radiology, 2019, 292, 365-373.	7.3	198
58	A Curriculum Learning Strategy to Enhance the Accuracy of Classification of Various Lesions in Chest-PA X-ray Screening for Pulmonary Abnormalities. Scientific Reports, 2019, 9, 15352.	3.3	12
59	<p>Assessment Of Changes In Regional Xenon-Ventilation, Perfusion, And Ventilation-Perfusion Mismatch Using Dual-Energy Computed Tomography After Pharmacological Treatment In Patients With Chronic Obstructive Pulmonary Disease: Visual And Quantitative Analysis</p> . International Iournal of COPD. 2019. Volume 14, 2195-2203.	2.3	8
60	Prediction of Treatment Response in Patients with Chronic Obstructive Pulmonary Disease by Determination of Airway Dimensions with Baseline Computed Tomography. Korean Journal of Radiology, 2019, 20, 304.	3.4	8
61	CT Image Conversion among Different Reconstruction Kernels without a Sinogram by Using a Convolutional Neural Network. Korean Journal of Radiology, 2019, 20, 295.	3.4	30
62	A Review of Three-Dimensional Printing Technology for Medical Applications. Journal of the Korean Society of Radiology, 2019, 80, 213.	0.2	3
63	Prediction of Pulmonary Function in Patients with Chronic Obstructive Pulmonary Disease: Correlation with Quantitative CT Parameters. Korean Journal of Radiology, 2019, 20, 683.	3.4	29
64	The Role of medical doctor in the era of artificial intelligence. Journal of the Korean Medical Association, 2019, 62, 136.	0.3	1
65	Application of deep learning–based computer-aided detection system: detecting pneumothorax on chest radiograph after biopsy. European Radiology, 2019, 29, 5341-5348.	4.5	58
66	Deep Learning Algorithm for Reducing CT Slice Thickness: Effect on Reproducibility of Radiomic Features in Lung Cancer. Korean Journal of Radiology, 2019, 20, 1431.	3.4	47
67	Deep Learning Applications in Chest Radiography and Computed Tomography. Journal of Thoracic Imaging, 2019, 34, 75-85.	1.5	90
68	Short-term Reproducibility of Pulmonary Nodule and Mass Detection in Chest Radiographs: Comparison among Radiologists and Four Different Computer-Aided Detections with Convolutional Neural Net. Scientific Reports, 2019, 9, 18738.	3.3	18
69	Noncontrast Chest Computed Tomographic Imaging of Obesity and the Metabolic Syndrome. Journal of Thoracic Imaging, 2019, 34, 126-135.	1.5	10
70	Cycleâ€consistent adversarial denoising network for multiphase coronary CT angiography. Medical Physics, 2019, 46, 550-562.	3.0	157
71	Hybrid Airway Segmentation Using Multi-Scale Tubular Structure Filters and Texture Analysis on 3D Chest CT Scans. Journal of Digital Imaging, 2019, 32, 779-792.	2.9	7
72	Improvement of fully automated airway segmentation on volumetric computed tomographic images using a 2.5 dimensional convolutional neural net. Medical Image Analysis, 2019, 51, 13-20.	11.6	75

#	Article	IF	CITATIONS
73	Clinical Utility of Quantitative CT Analysis for Fissure Completeness in Bronchoscopic Lung Volume Reduction: Comparison between CT and Chartisâ"¢. Korean Journal of Radiology, 2019, 20, 1216.	3.4	6
74	CT Evaluation for Clinical Lung Cancer Staging: Do Multiplanar Measurements Better Reflect Pathologic T-Stage than Axial Measurements?. Korean Journal of Radiology, 2019, 20, 1207.	3.4	6
75	Diagnostic performance of CT-guided percutaneous transthoracic core needle biopsy using low tube voltage (100 kVp): comparison with conventional tube voltage (120 kVp). Acta Radiologica, 2018, 59, 425-433.	1.1	17
76	MRI for solitary pulmonary nodule and mass assessment: Current state of the art. Journal of Magnetic Resonance Imaging, 2018, 47, 1437-1458.	3.4	35
77	Comparison of Shallow and Deep Learning Methods on Classifying the Regional Pattern of Diffuse Lung Disease. Journal of Digital Imaging, 2018, 31, 415-424.	2.9	78
78	Prediction of survival by texture-based automated quantitative assessment of regional disease patterns on CT in idiopathic pulmonary fibrosis. European Radiology, 2018, 28, 1293-1300.	4.5	35
79	Urinary desmosine is associated with emphysema severity and frequent exacerbation in patients with <scp>COPD</scp> . Respirology, 2018, 23, 176-181.	2.3	10
80	Development of a Computer-Aided Differential Diagnosis System to Distinguish Between Usual Interstitial Pneumonia and Non-specific Interstitial Pneumonia Using Texture- and Shape-Based Hierarchical Classifiers on HRCT Images. Journal of Digital Imaging, 2018, 31, 235-244.	2.9	17
81	Volume doubling time of lung cancer detected in idiopathic interstitial pneumonia: comparison with that in chronic obstructive pulmonary disease. European Radiology, 2018, 28, 1402-1409.	4.5	11
82	A Perlin Noise-Based Augmentation Strategy for Deep Learning with Small Data Samples of HRCT Images. Scientific Reports, 2018, 8, 17687.	3.3	43
83	Quantitative assessment of pulmonary vascular alterations in chronic obstructive lung disease: Associations with pulmonary function test and survival in the KOLD cohort. European Journal of Radiology, 2018, 108, 276-282.	2.6	20
84	A novel CT-emphysema index/FEV <sub>1</sub> approach of phenotyping COPD to predict mortality. International Journal of COPD, 2018, Volume 13, 2543-2550.	2.3	6
85	Quantitative CT Imaging in Chronic Obstructive Pulmonary Disease: Review of Current Status and Future Challenges. Journal of the Korean Society of Radiology, 2018, 78, 1.	0.2	8
86	Positive association between moderate altitude and chronic lower respiratory disease mortality in United States counties. PLoS ONE, 2018, 13, e0200557.	2.5	10
87	Identification of chronic obstructive pulmonary disease subgroups in 13 Asian cities. International Journal of Tuberculosis and Lung Disease, 2018, 22, 820-826.	1.2	3
88	An Ensemble Method for Classifying Regional Disease Patterns of Diffuse Interstitial Lung Disease Using HRCT Images from Different Vendors. Journal of Digital Imaging, 2017, 30, 761-771.	2.9	7
89	Evaluation of postoperative lung volume and perfusion changes by dual-energy computed tomography in patients with lung cancer. European Journal of Radiology, 2017, 90, 166-173.	2.6	13
90	Improvement in Ventilation-Perfusion Mismatch after Bronchoscopic Lung Volume Reduction: Quantitative Image Analysis. Radiology, 2017, 285, 250-260.	7.3	19

#	Article	IF	CITATIONS
91	The role of dual-energy computed tomography in the assessment of pulmonary function. European Journal of Radiology, 2017, 86, 320-334.	2.6	22
92	Doubling time of thymic epithelial tumours on CT: correlation with histological subtype. European Radiology, 2017, 27, 4030-4036.	4.5	25
93	Myocardial segmentation based on coronary anatomy using coronary computed tomography angiography: Development and validation in a pig model. European Radiology, 2017, 27, 4044-4053.	4.5	10
94	Added value of prone CT in the assessment of honeycombing and classification of usual interstitial pneumonia pattern. European Journal of Radiology, 2017, 91, 66-70.	2.6	25
95	Imaging of COPD. , 2017, , 87-127.		0
96	Securing safe and informative thoracic CT examinations—Progress of radiation dose reduction techniques. European Journal of Radiology, 2017, 86, 313-319.	2.6	14
97	Management of COPD: Is there a role for quantitative imaging?. European Journal of Radiology, 2017, 86, 335-342.	2.6	14
98	Assessment of regional emphysema, air-trapping and Xenon-ventilation using dual-energy computed tomography in chronic obstructive pulmonary disease patients. European Radiology, 2017, 27, 2818-2827.	4.5	22
99	Radiomics and its emerging role in lung cancer research, imaging biomarkers and clinical management: State of the art. European Journal of Radiology, 2017, 86, 297-307.	2.6	222
100	Deep Learning in Medical Imaging: General Overview. Korean Journal of Radiology, 2017, 18, 570.	3.4	834
101	Size variation and collapse of emphysema holes at inspiration and expiration CT scan: evaluation with modified length scale method and image co-registration. International Journal of COPD, 2017, Volume 12, 2043-2057.	2.3	9
102	Validation of a CT-guided intervention robot for biopsy and radiofrequency ablation: experimental study with an abdominal phantom. Diagnostic and Interventional Radiology, 2017, 23, 233-237.	1.5	28
103	Imaging Heterogeneity of COPD. , 2017, , 179-187.		0
104	A size-based emphysema severity index: robust to the breath-hold-level variations and correlated with clinical parameters. International Journal of COPD, 2016, Volume 11, 1835-1841.	2.3	8
105	Relationship between vitamin D-binding protein polymorphisms and blood vitamin D level in Korean patients with COPD. International Journal of COPD, 2016, 11, 731.	2.3	11
106	Threeâ€dimensional quadratic modeling and quantitative evaluation of the diaphragm on a volumetric CT scan in patients with chronic obstructive pulmonary disease. Medical Physics, 2016, 43, 4273-4282.	3.0	4
107	Assessment of Regional Xenon Ventilation, Perfusion, and Ventilation-Perfusion Mismatch Using Dual-Energy Computed Tomography in Chronic Obstructive Pulmonary Disease Patients. Investigative Radiology, 2016, 51, 306-315.	6.2	32
108	Vitamin D Deficiency Is Associated with Rapid Decline in Exercise Capacity in Male Patients with Chronic Obstructive Pulmonary Disease. Respiration, 2016, 91, 351-358.	2.6	6

#	Article	IF	CITATIONS
109	Texture-Based Automated Quantitative Assessment of Regional Patterns on Initial CT in Patients With Idiopathic Pulmonary Fibrosis: Relationship to Decline in Forced Vital Capacity. American Journal of Roentgenology, 2016, 207, 976-983.	2.2	59
110	Optimal threshold of subtraction method for quantification of air-trapping on coregistered CT in COPD patients. European Radiology, 2016, 26, 2184-2192.	4.5	23
111	Visual Assessment of Chest Computed Tomography Findings in Anti-cyclic Citrullinated Peptide Antibody Positive Rheumatoid Arthritis: Is it Associated with Airway Abnormalities?. Lung, 2016, 194, 97-105.	3.3	11
112	Perfusion- and pattern-based quantitative CT indexes using contrast-enhanced dual-energy computed tomography in diffuse interstitial lung disease: relationships with physiologic impairment and prediction of prognosis. European Radiology, 2016, 26, 1368-1377.	4.5	27
113	Functional and Prognostic Implications of the Main Pulmonary Artery Diameter to Aorta Diameter Ratio from Chest Computed Tomography in Korean COPD Patients. PLoS ONE, 2016, 11, e0154584.	2.5	14
114	Relationship of vitamin <scp>D</scp> status with lung function and exercise capacity in <scp>COPD</scp> . Respirology, 2015, 20, 782-789.	2.3	25
115	Quantitative Assessment of Global and Regional Air Trappings Using Non-Rigid Registration and Regional Specific Volume Change of Inspiratory/Expiratory CT Scans: Studies on Healthy Volunteers and Asthmatics. Korean Journal of Radiology, 2015, 16, 632.	3.4	9
116	Bronchoscopic lung volume reduction by endobronchial valve in advanced emphysema: the first Asian report. International Journal of COPD, 2015, 10, 1501.	2.3	13
117	The Prognostic Value of Residual Volume/Total Lung Capacity in Patients with Chronic Obstructive Pulmonary Disease. Journal of Korean Medical Science, 2015, 30, 1459.	2.5	37
118	Size-based emphysema cluster analysis on low attenuation area in 3D volumetric CT: comparison with pulmonary functional test. , 2015, , .		2
119	Detailed analysis of the density change on chest CT of COPD using non-rigid registration of inspiration/expiration CT scans. European Radiology, 2015, 25, 541-549.	4.5	40
120	Development of New End-Effector for Proof-of-Concept of Fully Robotic Multichannel Biopsy. IEEE/ASME Transactions on Mechatronics, 2015, 20, 2996-3008.	5.8	17
121	Triage for suspected acute Pulmonary Embolism: Think before opening Pandora's Box. European Journal of Radiology, 2015, 84, 1202-1211.	2.6	16
122	Comparison of a New Integral-Based Half-Band Method for CT Measurement of Peripheral Airways in COPD With a Conventional Full-Width Half-Maximum Method Using Both Phantom and Clinical CT Images. Journal of Computer Assisted Tomography, 2015, 39, 1.	0.9	7
123	Pharmacological treatment response according to the severity of symptoms in patients with chronic obstructive pulmonary disease. Journal of Thoracic Disease, 2015, 7, 1765-73.	1.4	1
124	The Value of CT for Disease Detection and Prognosis Determination in Combined Pulmonary Fibrosis and Emphysema (CPFE). PLoS ONE, 2014, 9, e107476.	2.5	33
125	Design and Kinematic Analysis of a New End-Effector for a Robotic Needle Insertion-Type Intervention System. International Journal of Advanced Robotic Systems, 2014, 11, 190.	2.1	7
126	Study Design and Outcomes of Korean Obstructive Lung Disease (KOLD) Cohort Study. Tuberculosis and Respiratory Diseases, 2014, 76, 169.	1.8	49

#	Article	IF	CITATIONS
127	Efficacy of Bronchoscopic Lung Volume Reduction by Endobronchial Valves in Patients with Heterogeneous Emphysema: Report on the First Asian Cases. Journal of Korean Medical Science, 2014, 29, 1404.	2.5	9
128	Clinical Utility of Computed Tomographic Lung Volumes in Patients with Chronic Obstructive Pulmonary Disease. Respiration, 2014, 87, 196-203.	2.6	6
129	Automatic Left and Right Lung Separation Using Free-Formed Surface Fitting on Volumetric CT. Journal of Digital Imaging, 2014, 27, 538-547.	2.9	6
130	Thoracic cavity segmentation algorithm using multiorgan extraction and surface fitting in volumetric CT. Medical Physics, 2014, 41, 041908.	3.0	8
131	Improved correlation between CT emphysema quantification and pulmonary function test by density correction of volumetric CT data based on air and aortic density. European Journal of Radiology, 2014, 83, 57-63.	2.6	20
132	Emphysematous phenotype is an independent predictor for frequent exacerbation of COPD. International Journal of Tuberculosis and Lung Disease, 2014, 18, 1407-1414.	1.2	30
133	Assessment of Perfusion Pattern and Extent of Perfusion Defect on Dual-Energy CT Angiography: Correlations between the Causes of Pulmonary Hypertension and Vascular Parameters. Korean Journal of Radiology, 2014, 15, 286.	3.4	9
134	Longitudinal Lung Volume Changes in Patients with Chronic Obstructive Pulmonary Disease. Lung, 2013, 191, 405-412.	3.3	10
135	CT findings of pulmonary non-tuberculous mycobacterial infection in non-AIDS immunocompromised patients: a case-controlled comparison with immunocompetent patients. British Journal of Radiology, 2013, 86, 20120209.	2.2	35
136	Thoracic Magnetic Resonance Imaging for the Evaluation of Pulmonary Emphysema. Journal of Thoracic Imaging, 2013, 28, 160-170.	1.5	4
137	Prediction of Postoperative Lung Function in Patients Undergoing Lung Resection. Investigative Radiology, 2013, 48, 622-627.	6.2	38
138	Chronic Obstructive Pulmonary Disease: Lobe-based Visual Assessment of Volumetric CT by Using Standard Images—Comparison with Quantitative CT and Pulmonary Function Test in the COPDGene Study. Radiology, 2013, 266, 626-635.	7.3	72
139	Exertional Desaturation as a Predictor of Rapid Lung Function Decline in COPD. Respiration, 2013, 86, 109-116.	2.6	35
140	Automatic reconstruction of the arterial and venous trees on volumetric chest CT. Medical Physics, 2013, 40, 071906.	3.0	24
141	Low-Dose Chest Computed Tomography With Sinogram-Affirmed Iterative Reconstruction, Iterative Reconstruction in Image Space, and Filtered Back Projection. Journal of Computer Assisted Tomography, 2013, 37, 610-617.	0.9	23
142	Severity of Systemic Calcified Atherosclerosis Is Associated With Airflow Limitation and Emphysema. Journal of Computer Assisted Tomography, 2013, 37, 743-749.	0.9	19
143	A support vector machine classifier reduces interscanner variation in the HRCT classification of regional disease pattern in diffuse lung disease: Comparison to a Bayesian classifier. Medical Physics, 2013, 40, 051912.	3.0	19
144	An Engineering View on Megatrends in Radiology: Digitization to Quantitative Tools of Medicine. Korean Journal of Radiology, 2013, 14, 139.	3.4	5

#	Article	IF	CITATIONS
145	Expert Opinion. Journal of Thoracic Imaging, 2012, 27, 6.	1.5	3
146	High-Resolution CT Scan Findings in Familial Interstitial Pneumonia Do Not Conform to Those of Idiopathic Interstitial Pneumonia. Chest, 2012, 142, 1577-1583.	0.8	63
147	A Pilot Trial on Pulmonary Emphysema Quantification and Perfusion Mapping in a Single-Step Using Contrast-Enhanced Dual-Energy Computed Tomography. Investigative Radiology, 2012, 47, 92-97.	6.2	34
148	Phenotyping of chronic obstructive pulmonary disease: heterogeneity and its clinical relevance. Current Respiratory Care Reports, 2012, 1, 189-198.	0.6	3
149	Analysis of perfusion defects by causes other than acute pulmonary thromboembolism on contrast-enhanced dual-energy CT in consecutive 537 patients. European Journal of Radiology, 2012, 81, e647-e652.	2.6	42
150	Fast and efficient lung disease classification using hierarchical one-against-all support vector machine and cost-sensitive feature selection. Computers in Biology and Medicine, 2012, 42, 1157-1164.	7.0	15
151	Quantitative assessment of change in regional disease patterns on serial HRCT of fibrotic interstitial pneumonia with texture-based automated quantification system. European Radiology, 2012, 23, 692-701.	4.5	44
152	Dual-Energy CT in Patients Treated with Anti-Angiogenic Agents for Non-Small Cell Lung Cancer: New Method of Monitoring Tumor Response?. Korean Journal of Radiology, 2012, 13, 702.	3.4	57
153	Radiation Dose Reduction of Chest CT with Iterative Reconstruction in Image Space - Part I: Studies on Image Quality Using Dual Source CT. Korean Journal of Radiology, 2012, 13, 711.	3.4	24
154	Radiation Dose Reduction of Chest CT with Iterative Reconstruction in Image Space - Part II: Assessment of Radiologists' Preferences Using Dual Source CT. Korean Journal of Radiology, 2012, 13, 720.	3.4	11
155	Response patterns to bronchodilator and quantitative computed tomography in chronic obstructive pulmonary disease. Clinical Physiology and Functional Imaging, 2012, 32, 12-18.	1.2	19
156	CT Densitometry of the Lung in Healthy Nonsmokers with Normal Pulmonary Function. Journal of the Korean Society of Radiology, 2012, 67, 341.	0.2	0
157	Microvascular Pulmonary Tumor Embolism Detected by Perfusion Images of Dual-Energy Computed Tomography. Tuberculosis and Respiratory Diseases, 2012, 72, 63.	1.8	0
158	Contributors of the Severity of Airflow Limitation in COPD Patients. Tuberculosis and Respiratory Diseases, 2012, 72, 8.	1.8	3
159	Tracheal morphology and collapse in COPD: Correlation with CT indices and pulmonary function test. European Journal of Radiology, 2011, 80, e531-e535.	2.6	16
160	Improved Correlation Between CT Emphysema Quantification And Pulmonary Function Test By Density Correction Of Volumetric CT Data Based On Air And Aortic Density. , 2011, , .		0
161	Isolated Right Pulmonary Artery Hypoplasia with Retrograde Blood Flow in a 68-Year Old Man. Tuberculosis and Respiratory Diseases, 2011, 71, 126.	1.8	4
162	Predictors of Pulmonary Function Response to Treatment with Salmeterol/fluticasone in Patients with Chronic Obstructive Pulmonary Disease. Journal of Korean Medical Science, 2011, 26, 379.	2.5	12

#	Article	IF	CITATIONS
163	Comparison of Clinico-Physiologic and CT Imaging Risk Factors for COPD Exacerbation. Journal of Korean Medical Science, 2011, 26, 1606.	2.5	15
164	Comparison of Usual Interstitial Pneumonia and Nonspecific Interstitial Pneumonia: Quantification of Disease Severity and Discrimination between Two Diseases on HRCT Using a Texture-Based Automated System. Korean Journal of Radiology, 2011, 12, 297.	3.4	25
165	Airway Measurement for Airway Remodeling Defined by Post-Bronchodilator FEV1/FVC in Asthma: Investigation Using Inspiration-Expiration Computed Tomography. Allergy, Asthma and Immunology Research, 2011, 3, 111.	2.9	31
166	Different therapeutic responses in chronic obstructive pulmonary disease subgroups. International Journal of Tuberculosis and Lung Disease, 2011, 15, 1104-1110.	1.2	11
167	Pulmonary artery pressure in chronic obstructive pulmonary disease without resting hypoxaemia. International Journal of Tuberculosis and Lung Disease, 2011, 15, 830-837.	1.2	7
168	Computed tomography findings in invasive pulmonary aspergillosis in non-neutropenic transplant recipients and neutropenic patients, and their prognostic value. Journal of Infection, 2011, 63, 447-456.	3.3	53
169	Evaluation of computer-aided detection and dual energy software in detection of peripheral pulmonary embolism on dual-energy pulmonary CT angiography. European Radiology, 2011, 21, 54-62.	4.5	77
170	Regional Context-Sensitive Support Vector Machine Classifier to Improve Automated Identification of Regional Patterns of Diffuse Interstitial Lung Disease. Journal of Digital Imaging, 2011, 24, 1133-1140.	2.9	10
171	Validation of the Lower Limit of Normal Diffusing Capacity for Detecting Emphysema. Respiration, 2011, 81, 287-293.	2.6	11
172	Dual-energy Computed Tomography Characterization of Solitary Pulmonary Nodules. Journal of Thoracic Imaging, 2010, 25, 301-310.	1.5	83
173	Xenon Ventilation Imaging Using Dual-Energy Computed Tomography in Asthmatics. Investigative Radiology, 2010, 45, 354-361.	6.2	84
174	Pulmonary Embolism Associated With Inferior Vena Cava Interruption. Journal of Thoracic Imaging, 2010, 25, W131-W132.	1.5	3
175	Xenon ventilation CT using dual-source and dual-energy technique in children with bronchiolitis obliterans: correlation of xenon and CT density values with pulmonary function test results. Pediatric Radiology, 2010, 40, 1490-1497.	2.0	63
176	Concept of minimal heart rate for each pitch value to avoid interpolation artifact when using dual-source CT: a phantom study. International Journal of Cardiovascular Imaging, 2010, 26, 103-109.	1.5	3
177	Radiological findings and clinical features of thoracic immunoglobulin G4-positive plasma cell granuloma: two cases. British Journal of Radiology, 2010, 83, e150-e153.	2.2	2
178	Dual-Energy CT for Assessment of the Severity of Acute Pulmonary Embolism: Pulmonary Perfusion Defect Score Compared With CT Angiographic Obstruction Score and Right Ventricular/Left Ventricular Diameter Ratio. American Journal of Roentgenology, 2010, 194, 604-610.	2.2	138
179	Slope of Emphysema Index: An Objective Descriptor of Regional Heterogeneity of Emphysema and an Independent Determinant of Pulmonary Function. American Journal of Roentgenology, 2010, 194, W248-W255.	2.2	32
180	Collateral Ventilation in a Canine Model with Bronchial Obstruction: Assessment with Xenon-enhanced Dual-Energy CT. Radiology, 2010, 255, 790-798.	7.3	19

JOON BEOM SEO

#	Article	IF	CITATIONS
181	Responses to inhaled long-acting beta-agonist and corticosteroid according to COPD subtype. Respiratory Medicine, 2010, 104, 542-549.	2.9	89
182	Feasibility of Automated Quantification of Regional Disease Patterns Depicted on High-Resolution Computed Tomography in Patients with Various Diffuse Lung Diseases. Korean Journal of Radiology, 2009, 10, 455.	3.4	31
183	Pulmonary Complication of Novel Influenza A (H1N1) Infection: Imaging Features in Two Patients. Korean Journal of Radiology, 2009, 10, 531.	3.4	33
184	Novel level-set based segmentation method of the lung at HRCT images of diffuse interstitial lung disease (DILD). Proceedings of SPIE, 2009, , .	0.8	1
185	Performance testing of several classifiers for differentiating obstructive lung diseases based on texture analysis at high-resolution computerized tomography (HRCT). Computer Methods and Programs in Biomedicine, 2009, 93, 206-215.	4.7	27
186	Development of an Automatic Classification System for Differentiation of Obstructive Lung Disease using HRCT. Journal of Digital Imaging, 2009, 22, 136-148.	2.9	36
187	Correction of lung boundary using the gradient and intensity distribution. Computers in Biology and Medicine, 2009, 39, 239-250.	7.0	8
188	CT scanning-based phenotypes vary with ADRB2 polymorphisms in chronic obstructive pulmonary disease. Respiratory Medicine, 2009, 103, 98-103.	2.9	29
189	Vascular endothelial growth factor levels in induced sputum and emphysematous changes in smoking asthmatic patients. Annals of Allergy, Asthma and Immunology, 2009, 103, 51-56.	1.0	11
190	Xenon ventilation CT using a dual-source dual-energy technique: dynamic ventilation abnormality in a child with bronchial atresia. Pediatric Radiology, 2008, 38, 1113-1116.	2.0	48
191	Quantitative Assessment of Emphysema, Air Trapping, and Airway Thickening on Computed Tomography. Lung, 2008, 186, 157-165.	3.3	194
192	Newly developed ulcer-like projection (ULP) in aortic intramural haematoma on follow-up CT: is it different from the ULP seen on the initial CT?. Clinical Radiology, 2008, 63, 201-206.	1.1	29
193	Radiological and clinical findings of pulmonary aspergillosis following solid organ transplant. Clinical Radiology, 2008, 63, 673-680.	1.1	42
194	Coronary Artery Anomalies: Classification and Electrocardiogram-Gated Multidetector Computed Tomographic Findings. Seminars in Ultrasound, CT and MRI, 2008, 29, 182-194.	1.5	14
195	Oxygen-enhanced Magnetic Resonance Imaging versus Computed Tomography. American Journal of Respiratory and Critical Care Medicine, 2008, 177, 1095-1102.	5.6	87
196	Xenon Ventilation CT with a Dual-Energy Technique of Dual-Source CT: Initial Experience. Radiology, 2008, 248, 615-624.	7.3	155
197	Radiologic and Clinical Findings of Behçet Disease: Comprehensive Review of Multisystemic Involvement. Radiographics, 2008, 28, e31.	3.3	127
198	Clinical Utility of Dual-Energy CT in the Evaluation of Solitary Pulmonary Nodules: Initial Experience. Radiology, 2008, 249, 671-681.	7.3	243

#	Article	IF	CITATIONS
199	Quantitatively Assessed Dynamic Contrast-Enhanced Magnetic Resonance Imaging in Patients With Chronic Obstructive Pulmonary Disease: Correlation of Perfusion Parameters With Pulmonary Function Test and Quantitative Computed Tomography. Investigative Radiology, 2008, 43, 403-410.	6.2	57
200	Incidental Cardiac and Pericardial Abnormalities on Chest CT. Journal of Thoracic Imaging, 2008, 23, 216-226.	1.5	20
201	Effect of various binning methods and ROI sizes on the accuracy of the automatic classification system for differentiation between diffuse infiltrative lung diseases on the basis of texture features at HRCT. Proceedings of SPIE, 2008, , .	0.8	4
202	Texture-Based Quantification of Pulmonary Emphysema on High-Resolution Computed Tomography: Comparison With Density-Based Quantification and Correlation With Pulmonary Function Test. Investigative Radiology, 2008, 43, 395-402.	6.2	93
203	Semi-Automatic Measurement of the Airway Dimension by Computed Tomography Using the Full-Width-Half-Maximum Method: a Study on the Measurement Accuracy according to the CT Parameters and Size of the Airway. Korean Journal of Radiology, 2008, 9, 226.	3.4	30
204	Semi-Automatic Measurement of the Airway Dimension by Computed Tomography Using the Full-With-Half-Maximum Method: a Study of the Measurement Accuracy according to the Orientation of an Artificial Airway. Korean Journal of Radiology, 2008, 9, 236.	3.4	23
205	3-T MRI: Usefulness for Evaluating Primary Lung Cancer and Small Nodules in Lobes Not Containing Primary Tumors. American Journal of Roentgenology, 2007, 189, 386-392.	2.2	54
206	Imaging of Marfan Syndrome: Multisystemic Manifestations. Radiographics, 2007, 27, 989-1004.	3.3	91
207	Thoracic Periaortic Fibrosis Mimicking Malignant Tumor: CT and18F-FDG PET Findings. American Journal of Roentgenology, 2007, 188, 345-347.	2.2	5
208	Acute and Chronic Complications of Aortic Intramural Hematoma on Follow-up Computed Tomography. Journal of Computer Assisted Tomography, 2007, 31, 435-440.	0.9	44
209	Performance comparison of classifiers for differentiation among obstructive lung diseases based on features of texture analysis at HRCT. , 2007, , .		5
210	Long-Term Predictors of Descending Aorta Aneurysmal Change in Patients With Aortic Dissection. Journal of the American College of Cardiology, 2007, 50, 799-804.	2.8	299
211	Early and Delayed Myocardial Enhancement in Myocardial Infarction Using Two-Phase Contrast-Enhanced Multidetector-Row CT. Korean Journal of Radiology, 2007, 8, 94.	3.4	14
212	Efficient liver segmentation using a level-set method with optimal detection of the initial liver boundary from level-set speed images. Computer Methods and Programs in Biomedicine, 2007, 88, 26-38.	4.7	100
213	The performance improvement of automatic classification among obstructive lung diseases on the basis of the features of shape analysis, in addition to texture analysis at HRCT. , 2007, , .		5
214	Assessment of Coronary Artery Bypass Graft Patency Using Multidetector Computed Tomography. Journal of the Korean Medical Association, 2007, 50, 127.	0.3	0
215	Myocardial enhancement pattern in patients with acute myocardial infarction on two-phase contrast-enhanced ECG-gated multidetector-row computed tomography. Clinical Radiology, 2006, 61, 417-422.	1.1	29
216	Differentiation of Recently Infarcted Myocardium from Chronic Myocardial Scar: The Value of Contrast-Enhanced SSFP-Based Cine MR Imaging. Korean Journal of Radiology, 2006, 7, 14.	3.4	12

#	Article	IF	CITATIONS
217	Novel Technique of Aortic Valve Repair. Korean Circulation Journal, 2006, 36, 140.	1.9	5
218	Effects of High-Resolution CT of the Lung Using Partial Versus Full Reconstruction on Motion Artifacts and Image Noise. American Journal of Roentgenology, 2006, 187, 618-622.	2.2	21
219	Radiographic and CT Findings of Thoracic Complications after Pneumonectomy. Radiographics, 2006, 26, 1449-1468.	3.3	75
220	Coronary Artery Anomalies: Classification and ECG-gated Multi–Detector Row CT Findings with Angiographic Correlation. Radiographics, 2006, 26, 317-333.	3.3	284
221	Novel technique of aortic valvuloplastyâ~†â~†â~†. European Journal of Cardio-thoracic Surgery, 2006, 29, 530-536.	1.4	32
222	Comparison of Transaxial Source Images and 3-Plane, Thin-Slab Maximal Intensity Projection Images for the Diagnosis of Coronary Artery Stenosis with Using ECG-Gated Cardiac CT. Korean Journal of Radiology, 2006, 7, 20.	3.4	9
223	Pulmonary Parenchymal Involvement of Low-Grade Lymphoproliferative Disorders. Journal of Computer Assisted Tomography, 2005, 29, 825-830.	0.9	38
224	Displaced aortic arch sign on chest radiographs: a new sign for the detection of a left paratracheal esophageal mass. European Radiology, 2005, 15, 936-940.	4.5	2
225	Variation of the size of pulmonary venous ostia during the cardiac cycle: optimal reconstruction window at ECC-gated multi-detector row CT. European Radiology, 2005, 15, 1441-1445.	4.5	30
226	Squalene aspiration pneumonia in children: radiographic and CT findings as the first clue to diagnosis. Pediatric Radiology, 2005, 35, 619-623.	2.0	31
227	Pericardial rupture and cardiac herniation after blunt trauma: a case diagnosed using cardiac MRI. British Journal of Radiology, 2005, 78, 447-449.	2.2	28
228	Histopathologic Pattern and Clinical Features of Rheumatoid Arthritis-Associated Interstitial Lung Disease. Chest, 2005, 127, 2019-2027.	0.8	406
229	Cardiac Perforation Caused by Acrylic Cement: A Rare Complication of Percutaneous Vertebroplasty. American Journal of Roentgenology, 2005, 185, 1245-1247.	2.2	71
230	Filling Defect in a Pulmonary Arterial Stump on CT After Pneumonectomy: Radiologic and Clinical Significance. American Journal of Roentgenology, 2005, 185, 985-988.	2.2	48
231	Assessment of Papillary Muscle Function in Patients with Inferior Wall Myocardial Infarction Using Doppler Tissue Imaging. Journal of the American Society of Echocardiography, 2005, 18, 815-820.	2.8	4
232	The Clinical Value about Pulmonary Tuberculosis of Indirect Chest Radiography in Physical Examination for Conscription. Tuberculosis and Respiratory Diseases, 2005, 59, 356.	1.8	0
233	Manganese dipyridoxyl diphosphate (MnDPDP)-enhanced magnetic resonance imaging of acute reperfused myocardial injury in a cat model: part I: comparison with pathologic examination. Investigative Radiology, 2005, 40, 49-55.	6.2	3
234	Manganese dipyridoxyl diphosphate (MnDPDP)-enhanced magnetic resonance imaging of acute reperfused myocardial injury in a cat model: part II: comparison with cine magnetic resonance imaging. Investigative Radiology, 2005, 40, 56-61.	6.2	4

#	Article	IF	CITATIONS
235	Paradoxical Embolism Detected on CT Angiography and Treated With Temporary Inferior Vena Cava Filtration and Anticoagulation. American Journal of Roentgenology, 2004, 183, 1244-1246.	2.2	3
236	Amyloidosis and Lymphoproliferative Disease in Sj??gren Syndrome. Journal of Computer Assisted Tomography, 2004, 28, 776-781.	0.9	113
237	MR Imaging of Reperfused Myocardial Infarction: Comparison of Necrosis-Specific and Intravascular Contrast Agents in a Cat Model. Radiology, 2003, 226, 739-747.	7.3	23
238	Primary Endobronchial Actinomycosis Associated with Broncholithiasis. Respiration, 2003, 70, 110-113.	2.6	18
239	Liquid-Crystal Display Monitors and Cathode-Ray Tube Monitors: A Comparison of Observer Performance in the Detection of Small Solitary Pulmonary Nodules. Korean Journal of Radiology, 2003, 4, 153.	3.4	21
240	Percutaneous Fine Needle Aspiration Biopsy for the Intrathoracic Lesions: What is the Meaning of Non-Diagnostic Results?. Journal of the Korean Radiological Society, 2003, 48, 401.	0.0	2
241	Efficacy of Pigtail Catheter Drainage in Patients with Thoracic Empyema or Complicated Parapneumonic Effusion. Tuberculosis and Respiratory Diseases, 2003, 54, 219.	0.2	2
242	Broncholithiasis: Review of the Causes with Radiologic-Pathologic Correlation. Radiographics, 2002, 22, S199-S213.	3.3	113
243	Detection of Simulated Chest Lesions by Using Soft-Copy Reading: Comparison of an Amorphous Silicon Flat-Panel–Detector System and a Storage-Phosphor System. Radiology, 2002, 224, 242-246.	7.3	24
244	Benign Bronchopulmonary Tumors: Radiologic and Pathologic Findings. Journal of Computer Assisted Tomography, 2002, 26, 784-796.	0.9	13
245	Intravascular Papillary Endothelial Hyperplasia of the Lung. Journal of Computer Assisted Tomography, 2002, 26, 362-364.	0.9	9
246	Tuberculosis in Patients with Myelodysplastic Syndromes. Clinical Radiology, 2002, 57, 408-414.	1.1	9
247	Superficial Endobronchial Lung Cancer: Radiologic-Pathologic Correlation. Korean Journal of Radiology, 2002, 3, 229.	3.4	12
248	Two-Dimensional Breath-Hold Coronary MR Angiography in Normal Adults. Journal of the Korean Radiological Society, 2002, 46, 321.	0.0	0
249	Diffuse Telangiectatic Type of Pulmonary Arteriovenous Malformation Diagnosed with CT Scan using Slab Maximum Intensity Projection Technique: A Case Report. Journal of the Korean Radiological Society, 2002, 47, 357.	0.0	0
250	The Diagnosis of Small Solitary Pulmonary Nodule: Comparison of Standard and Inverse Digital Images on a High-Resolution Monitor using ROC Analysis. Journal of the Korean Radiological Society, 2002, 47, 601.	0.0	0
251	Radiographic Findings of Miliary Tuberculosis: Difference in Patients with and those without Associated Acute Respiratory Failure. Journal of the Korean Radiological Society, 2002, 47, 351.	0.0	0
252	Atypical Pulmonary Metastases: Spectrum of Radiologic Findings. Radiographics, 2001, 21, 403-417.	3.3	363

#	Article	IF	CITATIONS
253	Evaluation of Tracheobronchial Diseases: Comparison of Different Imaging Techniques. Korean Journal of Radiology, 2000, 1, 135.	3.4	10
254	Pulmonary Metastases of Alveolar Soft-Part Sarcoma: CT Findings in Three Patients. Korean Journal of Radiology, 2000, 1, 56.	3.4	10
255	Digital Chest Radiography with a Selenium-Based Flat-Panel Detector Versus a Storage Phosphor System. American Journal of Roentgenology, 2000, 175, 1013-1018.	2.2	32
256	Pulmonary vasculitis: the spectrum of radiological findings British Journal of Radiology, 2000, 73, 1224-1231.	2.2	49
257	Pulmonary Tuberculoma Evaluated by Means of FDG PET: Findings in 10 Cases. Radiology, 2000, 216, 117-121.	7.3	314
258	Renal and pulmonary lymphangioleiomyomatosis: a case report. European Journal of Radiology, 2000, 36, 126-129.	2.6	4
259	B-Cell Lymphoma of Bronchus-Associated Lymphoid Tissue (BALT): CT Features in 10 Patients. Journal of Computer Assisted Tomography, 2000, 24, 30-34.	0.9	76
260	Factors Influencing Vascular and Hepatic Enhancement at CT: Experimental Study on Injection Protocol Using a Canine Model. Journal of Computer Assisted Tomography, 2000, 24, 400-406.	0.9	85
261	Right paratracheal air cysts in the thoracic inlet: clinical and radiologic significance American Journal of Roentgenology, 1999, 173, 65-70.	2.2	156
262	Mucoepidermoid Carcinoma of the Tracheobronchial Tree: Radiographic and CT Findings in 12 Patients. Radiology, 1999, 212, 643-648.	7.3	141
263	Shark Liver Oil-induced Lipoid Pneumonia in Pigs: Correlation of Thin-Section CT and Histopathologic Findings. Radiology, 1999, 212, 88-96.	7.3	10
264	Exogenous lipoid pneumonia: high-resolution CT findings. European Radiology, 1999, 9, 287-291.	4.5	52
265	Mucous Gland Adenoma of the Bronchus: CT Findings in Two Patients. Journal of Computer Assisted Tomography, 1999, 23, 758-760.	0.9	25
266	Experimentally induced pulmonary arterial occlusion with detachable balloon in pigs: Thin-section CT findings. Academic Radiology, 1998, 5, 822-831.	2.5	5
267	Benign obstruction of the hepatic inferior vena cava complicated by hepatocellular carcinoma: combined interventional management American Journal of Roentgenology, 1998, 170, 655-659.	2.2	8
268	Intratumoral Vascularity of Experimentally Induced VX2 Carcinoma. Investigative Radiology, 1998, 33, 39-44.	6.2	18
269	Detection of hypervascular nodular hepatocellular carcinomas: value of triphasic helical CT compared with iodized-oil CT American Journal of Roentgenology, 1997, 168, 219-224.	2.2	61
270	Neofissure after lobectomy of the right lung: radiographic and CT findings Radiology, 1996, 201, 475-479.	7.3	5

#	Article	IF	CITATIONS
271	Clear cell tumor of the lung American Journal of Roentgenology, 1996, 166, 730-731.	2.2	21